

Silhouette Mapping

Xianfeng Gu

Steven J. Gortler

Hugues Hoppe

Computer Science, Harvard Univ.

Microsoft Research

Leonard McMillan

Benedict J. Brown

Abraham D. Stone

MIT LCS Computer Graphics

CS, Harvard

Dept of Philosophy, Harvard

March 15, 1999

Harvard University, Computer Science Technical Report: TR-1-99

Abstract

Recent image-based rendering techniques have shown success in approximating detailed models using sampled images over coarser meshes. One limitation of these techniques is that the coarseness of the geometric mesh is apparent in the rough polygonal silhouette of the rendering. In this paper, we present a scheme for accurately capturing the external silhouette of a model in order to clip the approximate geometry.

Given a detailed model, silhouettes sampled from a discrete set of viewpoints about the object are collected into a silhouette map. The silhouette from an arbitrary viewpoint is then computed as the interpolation from three nearby viewpoints in the silhouette map. Pairwise silhouette interpolation is based on a visual hull approximation in the epipolar plane. The silhouette map itself is adaptively simplified by removing views whose silhouettes are accurately predicted by interpolation of their neighbors. The model geometry is approximated by a progressive hull construction, and is rendered using projected texture maps. The 3D rendering is clipped to the interpolated silhouette using stencil planes.

1 Introduction

In interactive 3D rendering there is a constant tension between model complexity and rendering speeds. Scenes with high geometric complexity are necessary for visual realism, but require high computational costs to achieve. This tension will not go away soon. To this end there has been considerable research into how to best use a given amount of rendering resources, and a number of successful approaches have been developed.

One such approach is level-of-detail rendering [18]. In this approach, more polygons are used for nearby objects than for distant objects, using more rendering resources where they produce the most visual impact. More complicated view based level of detail methods also use more polygons in the silhouette regions of models, since this typically produces the highest quality visual appearance [42, 20, 27].

Another such approach is texture mapping and its descendant image based rendering algorithms. In these methods, resources are used to create photometric appearances of high complexity using objects with low geometric complexity and fidelity.

Some of the most impressive results are obtained from systems that combine concepts from both of these approaches [6, 9, 24, 31, 41]. Cohen et al. [9] combine model simplification with texture and normal maps to produce objects with high visual complexity with modest rendering budgets. This combination of approaches works extremely well at representing the appearances of the interiors of objects. The one limitation of these approaches is that they do a poor job of displaying high quality silhouettes of objects, since they use a low polygon count. This is unfortunate since the appearance of the silhouette of an object is one of the strongest visual cues as to the shape of an object [23].

To address this problem we have developed a rendering system that ensures that objects are displayed with high resolution silhouettes, even when low resolution geometry is used to speed up rendering. Like Cohen et al., we use simplified geometry to describe the objects' shapes, and we use textures to create high visual complexity in the objects' interiors. In our system, we introduce a *silhouette clipping* algorithm to ensure that the low resolution geometry is only drawn in the screen region defined by a high resolution silhouette. Silhouette clipping is an alternative to the view based level of detail methods such as [20], that must dynamically create a model simplified for the current view. These methods are quite complicated, and for model consistency must generate high polygon counts in regions that are near but not on the silhouette.

The first challenge one must face in order to do silhouette clipping is a way of quickly constructing a high resolution silhouette for a given view. One could extract the silhouette dynamically by appealing to the high resolution geometry for each frame as done in [30, 16]. But these methods compute all silhouette curves that separate front-facing polygons from back-facing polygons. Some of these curves lie in the interior of the model, and can not be used for silhouette clipping. We must be able to quickly compute only the boundary silhouettes (defined below).

Our system accomplishes the construction of a high resolution silhouette by using a precomputed *silhouette map*. A silhouette map is a data structure completely independent of the original geometry that stores an explicit representation of the silhouette contour as seen from a discrete set of views. To obtain a silhouette for an arbitrary current view, three "nearby" silhouettes are extracted from this silhouette map. *Silhouette interpolation* is performed to create a silhouette for the current view. Thus, during the rendering of the current view, the data accessed and processed is on the order of the complexity of a silhouette contour, which is typically much less than the size of the high resolution model.¹

¹As a rule of thumb, if the high resolution model has n polygons, and is tessellated evenly, the silhouette contour is usually made up of $O(\sqrt{n})$ edges.

In some ways, the silhouette interpolation problem referred to above resembles the contour interpolation problem found in animation and morphing applications [38], which can be solved effectively with a number of ad hoc solutions. But silhouette interpolation is different from contour morphing in a few key ways. Silhouette contours routinely undergo complicated topological changes as the viewpoint changes [23], and thus a silhouette interpolation method must be able to handle such cases routinely. Moreover, when there is a sharp feature point on the object, that point may remain on the silhouette of the nearby views. During silhouette interpolation, these points should be considered to be “in correspondence”. Typical contour morphing algorithms would not guarantee this. We have therefore developed a novel silhouette interpolation based on the epipolar geometry of two views. Our method can handle topological changes, and it ensures that actual feature points on silhouettes are treated as being in correspondence. Moreover, unlike the many existing contour morphing methods, our silhouette interpolation algorithm has a clear geometric interpretation. It also guarantees that the resulting interpolated silhouette contour is conservative: it is guaranteed to lie outside the actual silhouette that would be observed from the current view.

For typical objects, the silhouettes can change rapidly in some region of view space, and slowly in others. This happens for both geometric and topological reasons.

In areas of low surface curvature, the silhouette (when seen in 3D) slips quickly across the surface as the view changes, while in areas of high curvature, the silhouette moves slowly across the surface. In the limit, at sharp edges, the silhouette doesn’t move at all as the view position changes, until some change in global geometric configuration occurs.

When one considers both internal and external silhouettes portions (see terminology below), the topological changes that can occur for a silhouette are well understood [23]. As the view changes, the silhouette topology remains unchanged until a singular view is reached. At such a view a catastrophe occurs, and the topology of the silhouette changes according to well defined rules. When one only considers external silhouettes, as we do, the topological changes that occur cannot be analyzed as easily. Nevertheless, it should be clear that in certain regions, the silhouette undergoes discontinuous changes and interpolation becomes more difficult.

To address both of these problems, we have developed a *silhouette map simplification* algorithm that adaptively samples the view space. As a result, we keep more silhouette information in regions of view space where the silhouettes change most rapidly.

In order to perform silhouette clipping on the approximate geometry, one must have an approximation that encloses a volume that is larger than the original geometry. To this end we have developed a *progressive hull* representation. This creates a nested family of approximating meshes with the property that each coarser mesh encloses the finer meshes. This representation is a variant of the progressive mesh representation [19] that uses linear programming to ensure the desired hull property.

Our silhouette map could also be used in cases where explicit high resolution geometry is not available, but high resolution silhouette information is. One such promising example is image based rendering. Extracting high quality depth information from images is a difficult problem; automatic (multi)stereo algorithms are notoriously unreliable, and even the heartiest of graduate students quickly tires from manually specifying the necessary correspondence points. In contrast,

the silhouette of an object can be extract from an image easily and with high accuracy.

Contributions

Our work has a number of distinct contributions

- We introduce the idea of silhouette clipping, to efficiently render low resolution geometric objects with high resolution silhouettes .
- We introduce the idea of a silhouette map, which is an auxiliary data structure that stores the silhouette appearance from a number of sampled viewpoints.
- We describe an algorithm for silhouette interpolation. This algorithm, which is based on epipolar geometry can handle topological changes, keeps sharp feature points in correspondence, and guarantees a silhouette which is outside the actual silhouette .
- We describe a greedy simplification algorithm that samples silhouette information most densely in regions of view space where the most changes occur.
- We describe a progressive hull data structure for representing a nested sequence of enclosing approximate geometries. This representation may have other uses such as collision detection.

Limitations

Our work has several limitations and thus directions where future work is required.

- Silhouette clipping can only be applied to external silhouettes . Internal silhouettes are generally not closed contours, and therefore cannot be used to create a clipping region. This results in visible artifacts where an object is self occluding. To solve this, some method for decomposing the original object into subobjects would be necessary.
- Our interpolation method is conservative. Given the silhouettes recorded at three viewpoints in space, our algorithm will produce a conservative silhouettes for any viewpoint on the triangle connecting the three vertices. The actual silhouette is guaranteed to lie within the interpolated silhouette , but is generally not on it. Our interpolation algorithm is based on the concept of visual hull, which is generally too conservative. In order to produce tighter silhouettes ideally would require higher order differential information about the surface at each point on the silhouettes .
- Our algorithm is local, in that it only uses the nearest three views to create the interpolation. While for some classes of contours it can be shown that this is optimal, in general there are cases where other farther views can improve the computation of the silhouettes of the visual hull. Further analysis is required.

- The algorithm described in section 5.1 is an interpolation algorithm and not an extrapolation algorithm. In order to compute correctly silhouettes that are not on a triangle (because the viewpoint has moved closer or farther from the object) would require explicit depth information at each point on the silhouettes, or a tetrahedralization of space. In practice we use a simple planar homography (section 5) which we have found to work adequately well in practice.
- Subdividing the intervals of a span into cliques requires correspondence between the intervals in the two views. Our heuristic for this can be incorrect if multiple topological changes have occurred between the two views. In practice, this is taken care of by our silhouette map simplification algorithm. In regions where correspondence is difficult, denser samples are used. Again more analysis would be useful here.

Preliminaries

Silhouettes

In order to help our discussion, we will introduce here a small amount of terminology. For a pin hole imaging model and a smooth surface, a silhouette is created when a ray with direction vector \vec{r} passing through the pin hole touches the surface at a point \mathbf{P} where the normal of the surface is orthogonal to the ray direction

$$\vec{r} \cdot \vec{n}_P = 0$$

The set of 3D points \mathbf{P} for which this is true is called the *contour generator*. The contour generator is generically made up of a set of smooth closed 3D contours on the surface [7]. The projection of the contour generator onto the image plane is called the *apparent contour*. The apparent contour is a 2D curve that can self intersect, and at some points (called cusps) it can be non-smooth. If we view the image of an opaque object, many parts of the apparent contour are occluded by other parts of the object. We call the unoccluded part of the apparent contour the *visible apparent contour*. For a non-convex object, the visible apparent contour consists of two parts, *external* and *internal*. The internal part projects onto the interior of the image of the opaque object while the external part projects onto the boundary of the opaque object. The external part forms the boundary between the projection of an object and its background; this is defined by a closed contour (possibly with holes). In our system we only deal with the external visible apparent contour which we will hereafter refer to simply as the silhouette. See Plate 4.

The Visual Hull

In order to understand the conservative nature of our algorithms we briefly review the concept of the visual hull. Researchers have used (external) silhouette information to carve away regions of 3D space where it is known that the object is not present. The result of this carving is a shape called the *visual hull* of the object [25]. The visual hull is generally not identical to the object (for

example in a concave surface region), nor is it identical to its convex hull. Visual hull methods are extremely robust compared to other vision algorithms. We use the concept of the visual hull to develop our interpolation algorithm.

Suppose that some original 3D geometry is viewed from a set of views V . In each view i , the silhouette s_i is formed by the boundary between the points interior and exterior to the object. For view i we create the cone-like volume vh_i defined by all the rays starting at the image’s point of view \mathbf{p}_i and passing through the interior points on its image plane. It is guaranteed that the actual 3D geometry must be contained in vh_i . This statement is true for all i and so the 3D geometry must be contained in the volume $vh_V = \bigcap_i vh_i$. As the size of V goes to infinity, and includes all possible views, vh_V converges to an approximate shape known as the visual hull vh_∞ of the original geometry. The visual hull is not guaranteed to be the same as the original geometry since concave region shapes can never be distinguished using silhouette information.

In practice, one must construct approximate visual hulls using only a finite number of views. Given the set of views V , the approximation vh_V is the best conservative geometry that one can achieve. (If one doesn’t require a conservative estimate, then better approximations are usually achievable by fitting higher order surface approximations to the observed data [5].)

As one uses more and more views, the resulting hull improves, and converges to vh_∞ . Interestingly though, when one is only concerned with predicting silhouettes and one plans to view the scene from some view v_t that lies in the triangle defined by three views v_1, v_2, v_3 , then the silhouette observed is typically not improved by including any views other than v_1, v_2, v_3 . In other words $sill(v_t, vh_{123}) \approx sill(v_t, vh_\infty)$. The reasons for this will be discussed below. This is an encouraging result, for it means that local computation can be optimal.

Computation of visual hulls with high resolution can be a tricky matter. The intersection of the volumes vh_i is done with some form of CSG. If the silhouettes are polygonal, then the CSG can be done using polyhedral CSG but this is very hard to do in a robust fashion. More typically the CSG is done using a discrete voxelization of space [34]. In these systems one is usually severely limited by the low voxel resolutions achievable. The silhouette interpolation algorithm we use in our system provides us with a conservative approximation of the silhouette $s_c \approx sill(v_i, vh_{123})$ without ever explicitly constructing any visual hull data structures whatsoever.

2 Relation to Previous Work

Level of Detail/Simplification

Several level-of-detail (LOD) techniques have been developed to adapt the complexity of a mesh to changing viewing parameters. The simplest approach is to precompute for a given model a set of view-independent approximating meshes at different resolutions (see survey in [18]). Then, a runtime LOD framework can switch between these approximations based on the distance of the model from the viewer.

A more elaborate approach is to locally adapt the resolution of the approximating mesh at run-

time based on its relation to the viewer. For instance, areas of the surface can be kept coarser if they are outside the view frustum, facing away from the viewer, or sufficiently far away. Methods for this so-called view-dependent LOD have been presented by Xia and Varshney [42], Hoppe [20], and Luebke and Erikson [27]. In particular, the view-dependent error metric of Hoppe [20] automatically induces more refinement near the silhouette of the mesh. However, a cascade of dependencies between refinement operations also causes further refinement to faces not exactly on the silhouette, thus increasing rendering load. Another limitation of the view-dependent LOD approach is that its efficiency relies on time-coherence of the viewing parameters. If the view jumps quickly from one frame to the next, more work must be expended in traversing the refinement hierarchy.

In contrast, with silhouette clipping, fewer polygons need to be rendered since accurate, anti-aliased silhouettes are obtained as a 2D post-process. Moreover, computational effort is concentrated on the visible contour.

Silhouettes

It has long been recognized that silhouettes are an important visual cue that humans use to determine shape and recognize objects [23]. In *Solid Shape* [22], Koenderink catalogues the topological changes that can occur in the apparent contour as the viewpoint changes continuously.

In the computational vision community there is a large body of work studying how shape information can be computed from silhouette data. Koenderink and VanDoorn describe some of the shape information that can be deduced from a single image [23]. Giblin and Weiss [14] describe how shape can be extracted from silhouette information from multiple views. This work has been extended in numerous ways. For example Cipolla and Blake [7] provide a thorough analysis of the relationship between differential changes in the apparent contour seen by a moving observer, and the first and second fundamental forms of the surface geometry. They also analyze of the epipolar correspondence between silhouettes which we use in our silhouette interpolation algorithm. Boyer and Berger show how three discrete views can be used to compute an approximate osculating paraboloid for each point on the contour generator [5]. Many more references are contained in those papers.

In computer graphics, silhouette information has been used to enhance the expressive renderings of 3D objects [30, 15, 16]. We use the silhouette information to create renderings with the appearance of high resolution.

There are also a number of algorithms described for extracting silhouettes from polyhedral models. Blyth et al. describe a multipass rendering algorithm [4]. This algorithm requires a complete traversal of the high resolution geometry and is not fit for our purposes. Markosian et al. [30] describe an algorithm for quickly extracting both internal and external silhouette edges from a polyhedral model using random sampling and view coherence. Gooch et al. [16] describe a hierarchical Gauss map for quickly rejecting edges that are not on the silhouette. These two methods compute the entire contour generator, and not the silhouette. As a result they can not be used directly for silhouette clipping.

Image Based Rendering

Recently there has been a strong effort to develop image based rendering algorithms. These algorithms render new views starting from image-like input and representations. They can allow for faster rendering than from traditional model representations, and can also allow the creation of models using photographs as input, without requiring the lengthy process of geometric modeling.

Work such as that of Debevec et al [11] has shown that one can extract low resolution geometry and combine this with images to give the appearance of high resolution. In particular, they discuss the concept of view dependent texture maps wherein different projective textures [40] are used depending on the view. This work was further developed in [12]. In our system we adopt a similar rendering approach and use view dependent projective textures mapped onto low resolution geometry.

Seitz and Dyer [37] present a view morphing algorithm to interpolate between two images. Their system is based on the idea that if two images are rectified (such that their image planes are parallel to each other and to the direction of motion), all parallax is horizontal and linear. As a result, view interpolation can be done for each scan line independently, and linear interpolation can be used to warp the pixel locations. After correspondences are manually entered, their method consists of an image rectification of the pair of images, followed by a linear interpolation, followed by an unrectification of the resulting image. We adopt a similar three-stage approach (rectify pair, warp, unrectify) to perform silhouette interpolation. We interpolate between three views using a series of two pairwise interpolations.

Pollard and Hayes [36] present an image based algorithm that performs image interpolation between three views without manually specified correspondence by performing edge extraction and edge matching. They interpolate between three views by using barycentric linear interpolation, which is correct in the special case of orthographic views.

The silhouette map data structure described in this paper has some similarities to the light field representation [28, 35]. A light field attempts to sample all of the photometric information about an object. This can be thought of as storing the set of *images* viewed from a 2D manifold (a plane); this is effectively a 4d set of data. A silhouette map stores only the silhouette *contour* information viewed from a 2D manifold (for example a sphere) of views; this is effectively a 3D set of data. As a result it can be much more compact.

In a light field representation, data on the (s, t, u, v) domain is sufficient to correctly reconstruct a new view from any point in free space. This is due to the 4d nature of its data structure. In contrast, from a silhouette map one can only truly interpolate new silhouette information for new views on the sampling surface (sphere). As one moves off the sampling surface, one cannot do proper interpolation without additional information, such as depth. In the absence of such information, we use a simple scaling heuristic.

When a new view is reconstructed from a light field, (quadrilinear) interpolation is performed parametrically in the (s, t, u, v) domain. Effectively, nearby images are superimposed on top of each other. As a result, if the light field sampling rate is low, and the underlying geometry non-planar, the result can have significant ghosting (or blurring) artifacts. Without depth information (or

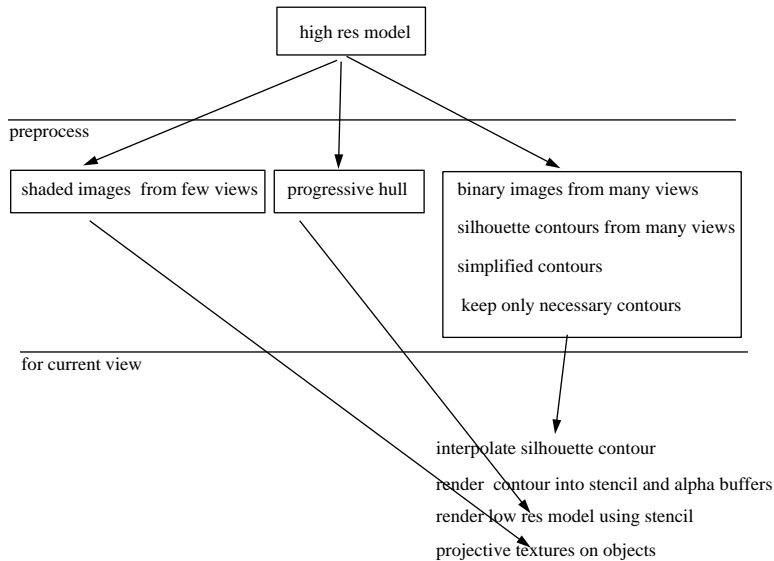


Figure 1: System overview.

its moral equivalent in some form) light field data cannot generally be interpolated or extrapolated very far. When interpolating from a silhouette map, the nearby silhouettes are interpolated in 2D geometrically, and so no ghosting can occur.

When reconstructing new views from a light field/lumigraph representation using geometric correction [35], one obtains a result very similar to view dependent texture mapping. No processing is done on the silhouettes, and so ghosting is still visible on the silhouettes (see Figure 17d of [35]).

Contour Morphing

Contour morphing is an animation technique that creates a smooth transition from one contour to another. Sederberg and Greenwood [38] describe a method that uses a toroidal shortest path approach to solve for a correspondence between points on two simple closed contours. Given such a correspondence, Sederberg et al. [39] use a turtle graphics metaphor to drive the interpolation of intermediate views. Shapira and Rappoport [29] use a star-skeleton decomposition of the contour to achieve higher quality animations. These methods provide no simple way to morph between two contours with differing topologies, and so it would be difficult to use these for silhouette interpolation. Cohen-Or et al. [10] use a distance field interpolation (similar in spirit to [21]) to interpolate between two arbitrary contours. Although this method can handle topology changes and is very useful for animation, for our purposes it would be a rather ad hoc choice. It is not based on the geometry of silhouette generation, has no geometric interpretation, no relation to the visual hull, and will not properly interpolate actual sharp feature points on a silhouette.

3 System Overview

An overview of our system is described in Figure 1. We begin with a high resolution polyhedral model as input. We first apply a number of preprocessing operations on the data. First we render a small number of views to be later used as textures to projectively map onto the rendered low resolution geometry. We select the views by hand using a simple interactive program. Automatic view selection would be desirable; this remains an open question.

Next a progressive hull construction is run on the high resolution geometry. The resulting progressive hull is a sequence of lower and lower resolution mesh geometries with the property that the volume defined in each successive lower resolution mesh is guaranteed to contain the volume defined by the previous higher resolution meshes. This property allows us to render views of the low resolution geometry which can be clipped to a high resolution silhouette.

Finally a silhouette map is constructed. To do this we render binary images of the object as seen from a large number of viewpoints on a surrounding sphere. A pixel-resolution polygonal contour is generated from each image; this contour is then simplified using a simplification algorithm similar to [19]. These contours make up a dense silhouette map. We run a silhouette map simplification algorithm to discard views that can be well predicted with the remaining views.

At run time for an arbitrary current view, we find three nearby views on the silhouette map, and an interpolated silhouette is produced. This new silhouette contour is drawn into the stencil buffer. Then the low resolution geometry is rendered using the stencil buffer to clip out the shape of the high resolution silhouette. A subset of the prerendered images are used as projective textures applied to the low res geometry. The result is a rendering with high resolution appearance.

4 Silhouette Map Representation

At the heart of our system is the silhouette map representation. The map represents the shape of the external visible apparent contour (silhouette) as seen from a number of views. A view v_i stores its intrinsic and extrinsic camera parameters including the location of the point of view \mathbf{p}_i . The view also stores the silhouette s_i seen from that view. The silhouette is represented as a closed polygon, possibly with holes.

The 3D positions of the optical centers of the view cameras form the vertices of some star shaped triangulated polytope that surrounds the object in question. See plate 6. This polytope is represented as a 3D mesh. The center of the polytope \mathbf{c} is also stored in the silhouette map. For an arbitrary current view point \mathbf{p}_c we form the segment connecting its position with the center of the polytope. If the viewpoint lies outside of the polytope, then this segment will intersect the polytope once in the interior of some triangle (or degenerately at some edge or vertex point). If the viewpoint lies inside of the polytope, the segment is extended backwards from the viewpoint until it intersects one of the polytope triangles. There is exactly one intersection because the polytope is star shaped. We call the intersection point on the triangle \mathbf{p}_t . The three views v_1, v_2, v_3 stored with the three vertices of the intersected triangle are called the “nearby views” and they are used

to generate the silhouette for the current view. This triangle intersection point \mathbf{p}_t can be tracked efficiently as the current view moves continuously by searching the neighborhood of the previous intersection point.

5 Silhouette Interpolation

Given three nearby views v_1, v_2, v_3 (at viewpoints $\mathbf{p}_1, \mathbf{p}_2, \mathbf{p}_3$) with their associated silhouettes s_1, s_2, s_3 , the goal of silhouette interpolation is to produce a silhouette s_c for the current view v_c taken from the viewpoint \mathbf{p}_c . Without 3D information about the silhouettes, this is a difficult problem and we make a number of approximations to make a solution feasible. In this section we describe our algorithm in detail, and discuss its geometric properties. The algorithm which must be invoked for each rendered frame runs in time $O(n \log n)$, where n is the number of vertices in the nearby silhouettes; this number is typically much less than the number of vertices in the original high resolution geometric model. The algorithm must create valid output even if the input silhouettes s_1, s_2, s_3 have different topologies.

We treat this problem in two steps. In the first step we use the interpolation method described below to produce an interpolated s_t for some view v_t that has \mathbf{p}_t (the intersection point in the triangle) as its viewpoint. In the second step we map s_t to the current view to produce the current silhouette s_c . During this second step we pretend that contour generator for s_t lies entirely in a plane that passes through the polytope center \mathbf{c} and is parallel to the triangle $\Delta(\mathbf{p}_1, \mathbf{p}_2, \mathbf{p}_3)$.² It is well known that the image of a planar object undergoes a 2D projective transformation as the view is changed. So we can model this transformation by applying a 3 by 3 matrix to all of the vertices of s_t to obtain s_c .

The following pseudocode shows an outline of the entire process. The remainder of this section discusses procedure `triSillInterp()`.

```
sill s_c <-- 3dSillInterp(view v_c, sillMap sm){
  (p_t, v_1, v_2, v_3) = polytopeIntersection(v_c, sm);
  (s_t, v_t) = triSillInterp(p_t, v_1, v_2, v_3, s_1, s_2, s_3);
  p_1 = v_1.pov; p_2 = v_2.pov; p_3 = v_3.pov;
  plane = planeThroughCenter(sm.center, p_1, p_2, p_3);
  H = determine3by3Matrix(plane, v_t, v_c);
  for each vertex index i in s_t
    s_c[i] = H * s_t[i];
  return s_c;
}
```

²This is an approximation since in general, the contour generator is not a plane curve at all [23]. And nearby points on the *external* visible apparent contour do not necessarily correspond to nearby points on the contour generator. Moreover, as one moves from \mathbf{p}_t to \mathbf{p}_c the points on the contour generator will generally not remain constant.

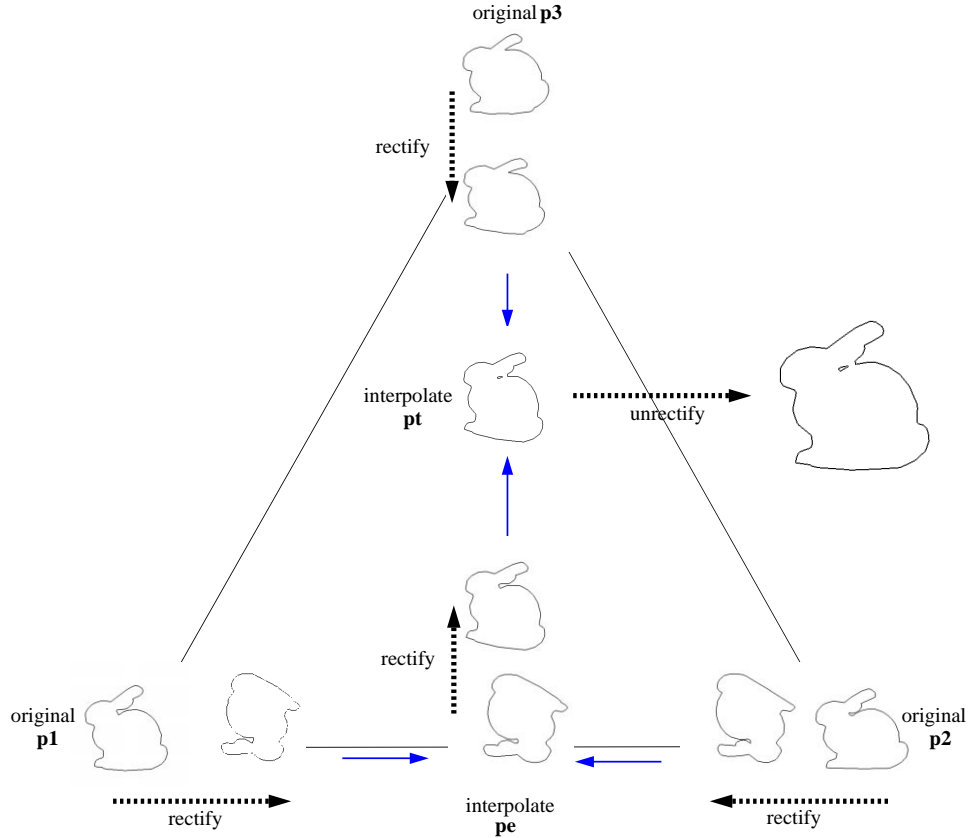


Figure 2: Triangular interpolation (in 2D).

5.1 Triangular Silhouette Interpolation

Given 3 views v_1, v_2, v_3 and their associated silhouettes s_1, s_2, s_3 and a point \mathbf{p}_t on the triangle $\mathbf{p}_1, \mathbf{p}_2, \mathbf{p}_3$ our goal is to produce the camera information for some view v_t with viewpoint \mathbf{p}_t on the triangle, and an interpolated silhouette s_t for that view.

In this section we describe our algorithm for this problem. Our algorithm has a number of unique features

- The algorithm runs in $O(n \log n)$ time.
- If a sharp point on the object is seen on the silhouettes of all the three nearby views, then the resulting interpolated silhouette s_t will correctly predict its location.
- The algorithm is conservative in way that is described below.
- The algorithm produces an interpolation with the above features even when the three input silhouettes have different topologies.

Briefly stated, we solve the triangular silhouette interpolation problem by solving two linear silhouette interpolation subproblems. In the linear silhouette interpolation algorithm we use the

epipolar geometry of the two views to rectify the two silhouettes, much as in the process of view morphing [37]. The vertices of the two rectified silhouettes are then processed in scan line order. Linear interpolation of the silhouette boundary is performed at the scan lines containing the vertices in order to produce an output set of vertices. Special care must be taken when the two silhouettes have a different number of spans on a given scan line. The resulting vertices are reconnected to create an output silhouette. The details and analysis follow.

Algorithm

Given three silhouettes from three views, finding the actual correspondence between points on these silhouettes is not a well defined problem. This is because as one’s view moves, the points on the contour generator slide locally over the surface. Only at points with infinite curvature (creases) do points on the contour generator remain constant; clearly at these points, the concept of actual correspondence is well defined, and should be obeyed by a silhouette interpolation algorithm. This problem is made even more difficult if the three silhouette polygons have different topologies³. Thus, barycentric coordinates cannot be directly used.

Given 2 silhouettes from 2 views, there is generally no actual physical correspondence. but there is a “natural” correspondence defined by the epipolar geometry of the two views, which has been used by vision researchers to extract curvature information from silhouettes [7, 14]. We use this epipolar correspondence to create an interpolation algorithm between two views with the desired criteria. Because this epipolar correspondence is only defined for pairs of views, and not triplets of views, we solve for s_c by solving a sequence of two pairwise interpolation steps.

First we find the edge of the triangle Δ_{123} that is closest to \mathbf{p}_t . Without loss of generality suppose this edge is defined by points $\mathbf{p}_1, \mathbf{p}_2$. We then find the the intersection \mathbf{p}_e of that edge and the line defined by \mathbf{p}_3 and \mathbf{p}_t . We perform linear silhouette interpolation between s_1 and s_2 to obtain the intermediate edge silhouette s_e . We then perform a second linear silhouette interpolation between s_3 and s_e to construct s_t . See Figure 2. We note that the result of this two-step interpolation is order-dependent.⁴

This is described by the following pseudocode:

```
(s_t, v_t) <-- triSillInterp(p_t, v_1, v_2, v_3, s_1, s_2, s_3){
  p_1 = v_1.pov; p_2 = v_2.pov; p_2 = v_2.pov;
  edge_12 = closestEdge((p_t, p_1, p_2, p_3); //wlog
  p_e      = isect(line(p_1,p_2), line(p_t, p_3) );
  (s_e, v_e) = linSillInterp(p_e, v_1, v_2, s_1, s_2);
  (s_t, v_t) = linSillInterp(p_t, v_e, v_3, s_3, s_3);
```

³At some singular viewpoints, the topology of the contour generator can change, and new closed contours can be created. At these viewpoints the apparent contour will change its topology. At other singular viewpoints, the topology of the contour generator may remain the same, but the topology of the (projected) apparent contour can change.

⁴As we will see below, each stage of linear silhouette interpolation will give us the same silhouette that is predicted by the the visual hull defined by the two input views (for example vh_{12}). But the composition of these two steps does not generate the same silhouette that would be predicted by the visual hull defined by all three views vh_{123} . It is only a conservative estimate. Further analysis is the topic of future research.

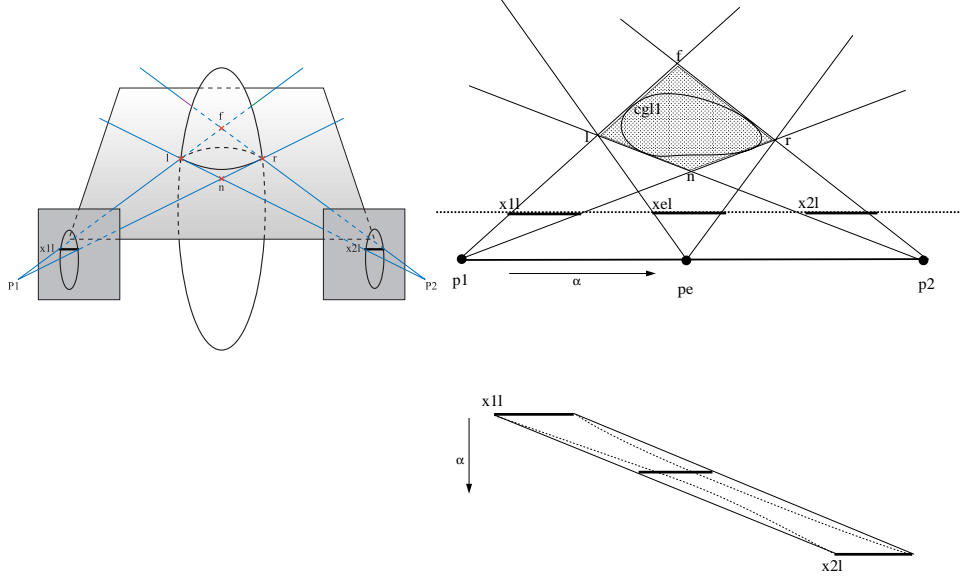


Figure 3: Silhouette interpolation in an epipolar plane.

```

return (s_t, v_t);
}

```

5.2 Linear Silhouette Interpolation

Given 2 views v_1, v_2 and their associated silhouettes s_1, s_2 and a point \mathbf{p}_e on the edge $\mathbf{p}_1, \mathbf{p}_2$ our goal is to produce the camera information for some view v_e with viewpoint \mathbf{p}_e , and an interpolated silhouette s_e for that view.

In this section we describe our algorithm for this problem. In addition to the above features, this step has the following property

- If span (defined below) correspondence is solved correctly then $s_e = sill(v_e, v_{h_{12}}) \approx sill(v_e, v_{h_\infty})$

As stated earlier, we wish to use an epipolar geometry to define correspondence. This will allow us to guarantee the above properties. In particular an epipolar decomposition of the scene will allow us to reduce the contour interpolation problem to a set of independent and much easier 1d span interpolation problem restricted to individual scan lines.

Epipolar Decomposition

Epipolar decomposition is most easily accomplished in a rectified domain. Given two silhouettes s_1, s_2 taken with 2 views v_1, v_2 with locations $\mathbf{p}_1, \mathbf{p}_2$ we construct the line $l = \overline{\mathbf{p}_1, \mathbf{p}_2}$. We then construct two new camera geometries v'_1, v'_2 such that their image planes are parallel to each other

and to l . We also require that the scan lines of the two image planes are aligned and in correspondence. We define the output view v_e to be a camera with center at \mathbf{p}_e and an image plane rectified with v'_1, v'_2 . This can be accomplished since all three camera centers lie on one line [37]. Because the views v_1 and v'_1 share the same camera center, one can correctly warp s_1 to s'_1 by computing the appropriate 3 by 3 matrix H_1 and applying it to the silhouette vertices. Likewise for v_2 .

In a rectified context, given some scan line s , there is an epipolar plane ep_s that includes the scan line s and the line l joining $\mathbf{p}_1, \mathbf{p}_2$. The intersection of ep_s and a closed 3D surface is generally a set of closed curves cr_s . If the epipolar plane intersects the top or bottom of a convex surface region, then the intersection can include unconnected points called frontier points [2]. See Plate 5.

The pin hole projection of the curves cr_s into the view v'_1 will cover a span sp_{1s} in scan line s . A span is defined by a set of covered intervals; this is described by an even number of vertices. Likewise, the pin hole projection of the curves cr_s into the view v'_2 will cover a span sp_{2s} in scan line s . Our strategy is to interpolate between sp_{1s} and sp_{2s} to produce a span sp_{es} in scan line s of the interpolated view v_e . If this can be done for all scan lines s , then we have accomplished our goal. Thus we have reduced a contour interpolation problem to a much easier span interpolation problem.

Algorithm

When the silhouettes are represented as polygons, and the scan line interpolation algorithm performs linear interpolation, the output silhouette will be a polygon with vertices at those scan lines where there are vertices in the original silhouettes. As a result, we do not need to apply our span interpolation algorithm at every scan line, but only at the scan lines where there are vertices. The algorithm thus resembles an active edge style polygon scan converter. The vertices of the rectified silhouettes, s'_1 and s'_2 , are sorted in y order. Scan lines that have vertices are visited from top to bottom. An active edge data structure allows us to quickly determine all of the edge intersects with the scan line. An interpolation is performed on the two spans, which results in an interpolated span. After all of the scan lines are processed, the resulting vertices are connected together to form the output silhouette ⁵.

```
(s_e, v_e) <-- linSillInterp(p_e, v_1, v_2, s_1, s_2){
  (v'_1, v'_2) = determineRectification(v_1, v_2);
  s'_1 = rectify(s_1, v_1, v'_1);
  s'_2 = rectify(s_2, v_2, v'_2);
  v_e = determineRectifiedEdgeView(p_e, v'_1, v'_2);

  sorted = sortVertsByYCoord(s_1, s_2);
  for each scanline s in sorted{
    sp_1s = intersect(s, s_1); //using active edge list
    sp_2s = intersect(s, s_2); //using active edge list
    sp_e[s] = spanInterp(v_e, v'_1, v'_2, sp_1s, sp_2s);
```

⁵Details of this step are not particularly enlightening and are deferred to a longer report.

```

}
s_e = connectUpSpans(sp_e);
return (s_e, v_e);
}

```

5.3 Span Interpolation

Given two rectified views v'_1, v'_2 , with two associated spans sp_{1s}, sp_{2s} the goal is to interpolate an output span sp_{es} for the view v_e . Because we are in a rectified context, this can be viewed entirely as a rectified problem in flatland(see Figure 3). This makes the problem much easier to analyze and solve.

Single Interval spans

The easiest case to consider (and the most frequent case) is when the epipolar plane ep_s intersects the 3D geometry in a single closed curve. In this case, the span seen from each of the two views v'_1, v'_2 will consist of a single covered interval (see Figure 3). The interval in v'_1 is defined by the two image x coordinate numbers $x1l, x1r$, and the interval in v'_2 is defined by the two numbers $x2l, x2r$.

In this case we use simple linear interpolation to predict the output interval (xel, xer).

$$\begin{aligned}
xel &= (1 - \alpha)x1l + (\alpha)x2l \\
xer &= (1 - \alpha)x1r + (\alpha)x2r
\end{aligned}$$

Where α represents the fraction of the distance along the segment.

It is well known (see for example [37]), that in a rectified context, linear interpolation of an image x coordinate between two views in image space (for example $(x1l, x2l)$) corresponds to the projection of some geometric point \mathbf{l} in space. The point \mathbf{l} must project in v'_1 with x coordinate $x1l$ and in v'_2 with $x2l$. Clearly \mathbf{l} must be the intersection in space between the ray from \mathbf{p}_1 passing through the left of the span on its image plane, and the ray from \mathbf{p}_2 passing through the left of the span on its image plane, Likewise for \mathbf{r} .

The linear interpolation algorithm behaves as if the silhouette was defined by fixed feature points \mathbf{l}, \mathbf{r} on the epipolar plane. This of course is not how the actual silhouette would behave on the curved surface. In the bottom of Figure 3, the dotted curves show the evolution of the actual silhouette while the solid lines show the evolution we predict. The velocity of the actual left point on the contour generator $\mathbf{cgl1}$ as one moves from v'_1 to v'_2 is governed by the following equation [7]

$$\frac{d\mathbf{cgl1}}{d\alpha} = \left(\frac{d\vec{r}}{d\alpha} \cdot \vec{n} \right) \vec{r} \quad (1)$$

where $\vec{r} = \frac{\mathbf{cgl1} - \mathbf{p}_1}{\|\mathbf{cgl1} - \mathbf{p}_1\|}$ is the direction from the optical center towards the contour generator, \vec{n} is the surface normal, and κ is the normal curvature (at the point $\mathbf{cgl1}$) of cr_s , the curve defined by the

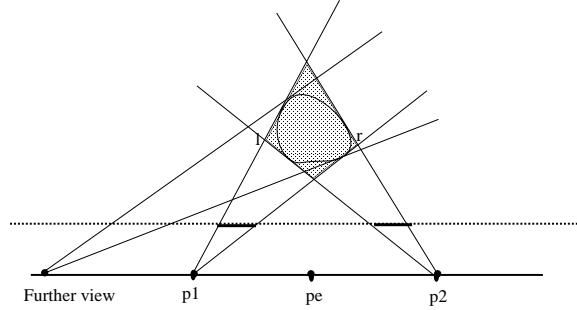


Figure 4: Further views dont help.

intersection of the 3D geometry with the epipolar plane . When the curvature is very low, the `cg11` slips quickly across the curve. When the curvature is high, the point slips slowly. In the limit, at a feature point with infinite curvature, the point on the contour generator does not move at all. In this case, if the same feature point is visible in both views, the linear interpolation algorithm will produce the correct prediction.

If we do not have an estimate of the curvature, the most conservative estimate is to assume it is a sharp point. This is exactly what our interpolation algorithm does. This is the same assumption that is made when constructing the visual hull.

If we were to explicitly construct the flatland visual hull vh_{12} from the given silhouette information, we would intersect the two associated wedges (flatland cones), giving us a quadrilateral surrounding the closed curve. The quadrilateral is defined by four points in space l, r, n, f (left, right, near and far). For any view v_e that lies on the segment connecting v'_1, v'_2 , the flatland observed silhouette $sill(v_e, vh_{12})$ is a single interval defined by the projection of the two points l, r into v_e . In fact, it can easily be proven that given more silhouettes observed from a set of views V where the extra viewpoints lie on the line l but outside of the the segment $\overline{p_1 p_2}$, that $sill(v_e, vh_{12}) = sill(v_e, vh_V)$. In other words, having more silhouette information from farther away than the surrounding two views cannot improve the predicted silhouette ⁶. See Figure 4.

To summarize, in the case of a closed curve, the linear interpolation of the interval endpoints is equivalent to predicting the silhouette using vh_{12} . Using views from farther away can not improve this prediction.

Multiple Interval Spans: Pants

When the intersection of the epipolar plane and the 3D geometry consists of more than one closed curve, the situation gets a bit more complicated. In this case the span in each view can be made up of any number of intervals, and the number of intervals in the two views need not be the same. For example in Figure 5, the left span has one interval, and the right span has two intervals. If one draws the actual evolution of the observed silhouette intervals as one moves from p_1 to p_2 using the vertical dimension as time, α , one obtains the diagram shown as dotted curves in Figure 5.

⁶A formal proof is left to a longer report.

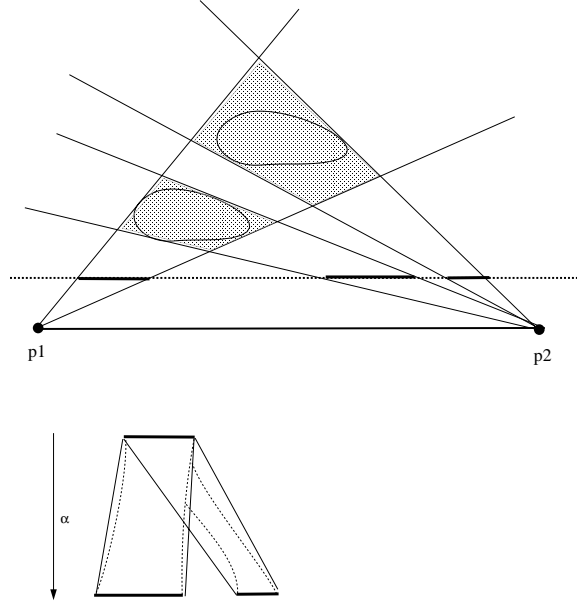


Figure 5: Pants.

Clearly this exact shape would be hard to predict simply from the silhouette information in the two views.

Once again we appeal here to vh_{12} , which in the case of Figure 5 is made up of two quadrilaterals. The evolution of the silhouette of the visual hull is defined by the solid lines in the figure, a configuration we refer to as “pants”. The pants evolution can also be correctly predicted using a modified linear interpolation algorithm.

Given that the left view span has a single interval x_{1l}, x_{1r} and the right view has two spans x_{2la}, x_{2ra} and x_{2lb}, x_{2rb} one performs the following pants computation

```

xela = lerp(alpha, x1l, x21a);
xera = lerp(alpha, x1r, x2ra);
xelb = lerp(alpha, x1l, x21b);
xerb = lerp(alpha, x1r, x2rb);
if (xelb < xera)
    return (xela, xerb);
else
    return (xela, xera, xelb, xerb);

```

In the case $x_{elb} < x_{era}$ the image of the two quadrilaterals in vh_{12} overlap in the output view, and only one interval is output. Otherwise, the image includes 2 intervals which are output. In either case, the correct visual hull is reproduced.

We note that in the case of multiple intervals, it is not the case that one will not be helped by silhouette information from farther views, i.e., $sill(v_e, vh_{12}) \neq sill(v_e, vh_V)$. For example see Figure 6. For efficiency, in this case we still do not use more views, and understand that our

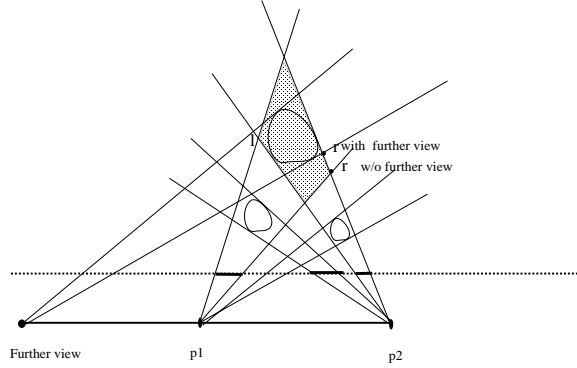


Figure 6: Further views do help.

prediction may be suboptimal.

Mutant Pants

The pants algorithm can be extended in a straightforward manner to include more complicated topological changes such as n -legged pants, and two-sided-no-torso pants (see Figure 8).

In Figure 7, we show an example where both the left and right views have spans with two intervals. The visual hull here is defined by the four shaded quadrilaterals, which results in two sided pants. If there is no geometry in the front and back quadrilaterals, then this is overly conservative. If we can determine that during the interpolation, the two observed silhouette intervals do not interact, then we can use the less conservative interpolation shown on the right. More generally given n intervals for v'_1 , and m intervals for v'_2 , we attempt to group the intervals in into cliques such as those shown in in Figure 8. An independent pants is created for each clique.

We have developed a heuristic algorithm for clique determination using the matching of frontier points and tracking from span to span. Stated briefly, for the pair of views, we attempt to form a correspondence between the convex and concave minima and maxima of the silhouette. Matched extrema, and their associated spans are put in separate cliques. Unmatched extrema and their associated spans are put in the nearest existing clique. This heuristic works well if the views are taken closely together with few topological changes between the views. An adequate sampling rate is set adaptively by the silhouette map simplification algorithm described next.

6 Silhouette Map Simplification

In a silhouette map, views are sampled at a set of vertices describing a star-shaped polytope surrounding the object. For most objects, a uniform sampling is inefficient. In some regions of view space, the silhouette changes slowly (for example κ in equation 1 may be large). In other regions, the silhouette may change rapidly. Geometrically this can occur where k is small. Moreover when topological changes occur, our interpolation algorithm uses the pants connection, which can be

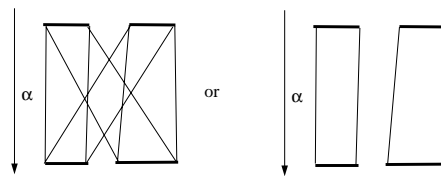
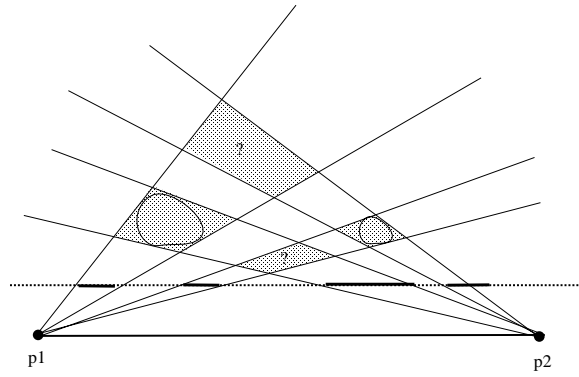


Figure 7: Two different possible hulls.

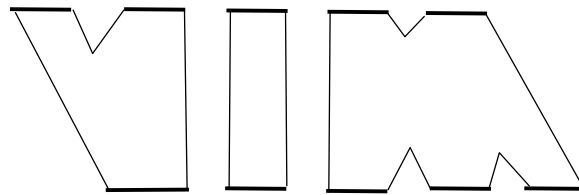


Figure 8: Cliques with mutant pants.

quite conservative, making a higher sampling rate desirable. Our solution to this is to use an adaptive sampling in the silhouette map. This is achieved using a greedy silhouette map simplification procedure that is inspired by the mesh simplification algorithm described in [19].

In particular, we begin with a silhouette map that contains many samples, densely surrounding the object. It is this original data that any simplified map must approximate. During the simplification process, any edge on the silhouette map polytope can be collapsed and one of its views discarded. We associate with each edge the error that would be incurred by collapsing it. The error is measured by comparing the original silhouette data points with predictions that would be made by the simplified mesh. The error metric measures the number of pixels that are misclassified (interior/exterior) by the prediction. Since we wish the polytope to remain star shaped, an edge is given infinite cost if its collapse would lead to a non-star shape.

The edges are stored in a heap, sorted by cost. The lowest cost edge is removed from the heap, and is collapsed in the silhouette map. The edges in the neighborhood of the collapse must then have their costs reevaluated.

An example of the simplification is shown in Plate 6. The simplification is somewhat time

consuming, and is run as a preprocess.

7 Construction of progressive hulls

For the rendering application in this paper, we need to compute, for an arbitrary triangle mesh M^n , a set of one or more coarser approximating meshes that completely enclose M^n . In this section, we solve the somewhat more general problem of constructing from M^n a continuous family of nested approximating meshes $M^0 \dots M^n$, such that

$$\mathcal{V}(M^0) \supseteq \mathcal{V}(M^1) \dots \supseteq \mathcal{V}(M^n)$$

where $\mathcal{V}(M)$ denotes the interior volume of M . We refer to $\{M^0 \dots M^n\}$ as a *progressive hull* (PH) sequence for M^n . Before presenting the technique in more detail, let us first more precisely define $\mathcal{V}(M)$.

Definition of interior volume The given mesh M^n is assumed to be orientable and closed (i.e. it has no boundaries). The mesh may have several connected components, and may contain interior cavities (e.g. a hollowed sphere). In most cases, it is relatively clear which points lie in the interior volume $\mathcal{V}(M)$. The definition of interior is less obvious in the presence of self-intersections, or when surfaces are nested (e.g. concentric spheres). Interfaces for 2D rasterization often allow several rules to define the interior of non-simple polygons [1, 32]. These rules do generalize to the case of meshes in 3D, as shown next.

To determine if a point $\mathbf{p} \in \mathbf{R}^3$ lies in the interior of a mesh M , select a ray from \mathbf{p} off to infinity, and find all intersections of the ray with M . Assume without loss of generality that the ray intersects the mesh only within interiors of faces (i.e. not on any edges). Each intersection point is assigned a number, +1 or -1, equal to the sign of the dot product between the ray direction and the normal of the intersected face. Let the *winding number* $w_M(\mathbf{p})$ be the sum of these numbers. Because the mesh is closed, it can be shown that $w_M(\mathbf{p})$ is independent of the chosen ray.

Based on $w_M(\mathbf{p})$, several definitions of interior volume are possible. The *non-zero* winding rule defines \mathbf{p} to be interior if and only if $w_M(\mathbf{p}) \neq 0$. With the *even-odd* rule, the condition is that $w_M(\mathbf{p})$ is odd. In this work, we use the *positive winding rule* which defines interior volume as

$$\mathcal{V}(M) = \{\mathbf{p} \in \mathbf{R}^3 : w_M(\mathbf{p}) > 0\} .$$

Progressive mesh representation The progressive hull (PH) sequence is an adaptation of the earlier *progressive mesh* (PM) representation [19] developed for level-of-detail control and progressive transmission of geometry.

The PM representation of a mesh M^n is obtained by simplifying the mesh through a sequence of *edge collapse* transformations, and recording their inverses. Specifically, the PM representation consists of a coarse base mesh M^0 and a sequence of n *vertex split* transformations (Figure 9) that

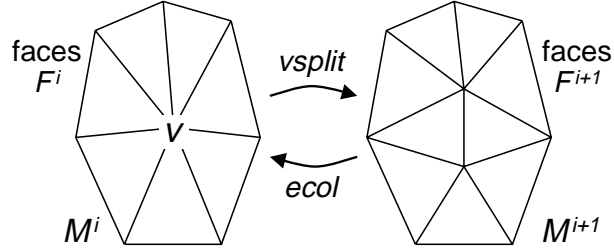


Figure 9: The vertex split transformation and its inverse, the edge collapse transformation.

progressively recover detail. Thus, the representation captures a continuous family of approximating meshes $M^0 \dots M^n$.

As shown in Figure 9, each edge collapse transformation unifies two adjacent vertices into one, thereby removing two faces from the mesh. For the purpose of level-of-detail control, edge collapses are selected so as to best preserve the appearance of the mesh during simplification. Several appearance metrics have been developed (e.g. [9, 13, 17, 19, 26]).

In this paper, we show that proper constraints on the selection of edge collapse transformations allow the creation of PM sequences that are progressive hulls.

Progressive hull construction For the PM sequence to be a progressive hull, each edge collapse transformation $M^{i+1} \rightarrow M^i$ must satisfy the property

$$\mathcal{V}(M^i) \supseteq \mathcal{V}(M^{i+1}) .$$

A sufficient condition is to guarantee that, at all points in space, the winding number either remains constant or increases:

$$\forall \mathbf{p} \in \mathbf{R}^3 , w_{M^{i+1}}(\mathbf{p}) \geq w_{M^i}(\mathbf{p}) .$$

Intuitively, the surface must either remain unchanged or locally move “outwards” everywhere.

Let F^i and F^{i+1} denote the sets of faces in the neighborhood of the edge collapse as shown in Figure 9, and let \mathbf{v} be the position of the unified vertex in M^i . For each face $f \in F^{i+1}$, we constrain \mathbf{v} to lie “outside” the plane containing face f . Note that the outside direction from a face is meaningful since the mesh is oriented. The resulting set of linear inequality constraints defines a feasible volume for the location of \mathbf{v} . The feasible volume may be empty, in which case the edge collapse transformation is disallowed. The transformation is also disallowed if either F^i or F^{i+1} contain self-intersections.⁷ If \mathbf{v} lies within the feasible volume, it can be shown that the faces F^i cannot intersect any of the faces F^{i+1} . Therefore, $F^i \cup flip(F^{i+1})$ forms a simply connected, non-intersecting, closed mesh enclosing the difference volume between M^i and M^{i+1} . The winding number $w(\mathbf{p})$ is increased by 1 within this difference volume and remains constant everywhere else. Therefore, $\mathcal{V}(M^i) \supseteq \mathcal{V}(M^{i+1})$.

The position \mathbf{v} is found with a linear programming algorithm, using the above linear inequality constraints and the goal function of minimizing volume. Mesh volume, defined here

⁷We currently hypothesize that preventing self-intersections in F^i and F^{i+1} may be unnecessary.

as $\int_{\mathbf{p} \in \mathbf{R}^3} w_M(\mathbf{p}) d\mathbf{p}$, is a linear function on \mathbf{v} that involves the ring of vertices adjacent to \mathbf{v} (refer to [17, 26]).

As in earlier simplification schemes, all candidate edge collapses are entered into a priority queue according to some cost metric. At each iteration, the edge with the lowest cost is collapsed, and the costs of affected edges are recomputed. Various cost metrics are possible. To obtain monotonically increasing bounds on the accuracy of the hull, one can track maximum errors as in [3, 8]. Another choice is the quadric error metric [13]. We obtain good results simply by minimizing the increase in volume, which matches the goal function used in positioning the vertex.

As discussed in Section 8.2, each projected texture used in rendering a coarse mesh M^c requires a surface parametrization. A simple approach is to map the positions of vertices in M^c through the same projective view that captured the image. Because the mesh M^c is an outer hull of the original mesh M^n , its vertices may lie some distance from M^n . We have found that the parametrization is improved if we associate to each vertex \mathbf{v} in M^c a “closest point” $\mathcal{P}(\mathbf{v})$ on the surface of M^n . We set $\mathcal{P}(\mathbf{v}) = \mathbf{v}$ for all $\mathbf{v} \in M^n$, and for each edge collapse $M^{i+1} \rightarrow M^i$, assign to the unified vertex $\mathbf{v} \in M^i$ the parametrization $\mathcal{P}(\mathbf{p})$ linearly interpolated at its closest point \mathbf{p} on the surface of M^{i+1} .

Inner and outer hulls The algorithm described so far constructs a *progressive outer hull* sequence $\overline{M}^0 \supseteq \dots \supseteq \overline{M}^n$. By simply reversing the orientation of the initial mesh M^n , the same construction gives rise to an *progressive inner hull* sequence $\underline{M}^0 \subseteq \dots \subseteq \underline{M}^n$. Combining these produces a single sequence of hulls

$$\underline{M}^0 \subseteq \dots \subseteq \underline{M}^n = \overline{M}^n \subseteq \dots \subseteq \overline{M}^0$$

that bounds the mesh M^n from both sides.

We expect that this representation will also find useful applications in collision detection, particularly using a selective refinement framework [20, 42].

8 Rendering Using Silhouette Clipping

To exploit the computed polygonal silhouette, we structure the rendering process as follows. First, we draw the silhouette polygon into the stencil plane of the frame buffer, setting the stencil bits at each pixel such that future rendering operations only affect the interior of the silhouette polygon. Second, we render the coarse mesh subject to the stencil, mapping textures onto the mesh faces using the precomputed object views. Finally, to obtain an anti-aliased silhouette, we render the silhouette polygon as an anti-aliased polyline, recording the alpha values in the frame buffer. We then render the coarse mesh again, using those computed alpha values at the silhouette pixels. We next describe each of these steps in further detail.

8.1 Silhouette clipping

At each frame, the stencil plane is initialized to zero as part of the frame buffer clear operation. Even though the silhouette polygon is generally concave and contains holes, it can be rasterized into the stencil plane efficiently as a single triangle fan. The trick is to use parity bits so that overlapping triangles cancel out correctly; for details, refer to the OpenGL programming guide [33]. Note that drawing the silhouette polygon is a simple 2D rasterization operation and is thus extremely fast. Having established the silhouette in the stencil plane, we next render the coarse mesh subject to the stencil.

8.2 Projective textures

In a precomputation stage, we store a small number of shaded images of the high resolution geometry as textures. For each face of the coarse mesh, we compute the set of texture views from which it is completely visible [12]. This set of visible textures is stored as a visibility bit vector associated with the face.

During rendering we sort the texture views in order of increasing distance from the current camera view, where distance is simply Euclidean distance between the camera centers. The number of texture views is generally small (e.g. 20) so this sorting operation is fast. For each face of the coarse mesh, the texture used to texture map the face is taken to be the closest texture view that is contained in the visibility bit vector.

At each vertex of the face, the projective texture coordinates are obtained by projecting a 3D position into the appropriate texture view. While we could simply use the position of the vertex, texture map distortion is reduced by instead using the parametrizations $\mathcal{P}(\mathbf{v})$ computed in Section 7.

8.3 Anti-aliasing of the silhouette

One benefit of the silhouette clipping approach is that the silhouette can be anti-aliased even if the hardware lacks polygonal anti-aliasing. To achieve this, the silhouette polygon is rendered again simply as a 2D anti-aliased polyline, but only affecting the alpha channel of the frame buffer. Then, the mesh is rendered, using the alpha values already in framebuffer.

As with conventional polygonal rendering, correct anti-aliasing in the presence of multiple objects requires that the objects be rendered in back-to-front order.

9 Results

Plate 1 shows meshes in a progressive hull sequence for a mesh of 69,674 faces. Construction of the sequence took 17 minutes on an SGI R10K, but the prototype software was not designed for

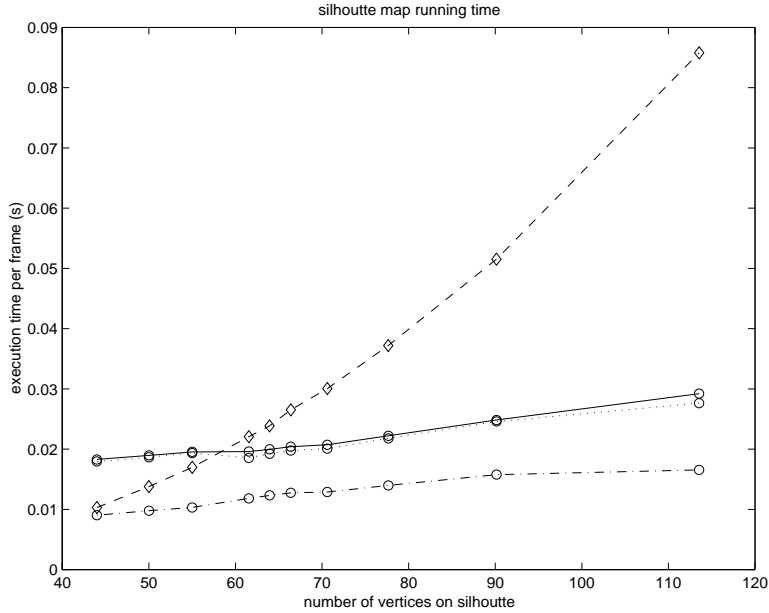


Figure 10: Rendering speeds.

speed. Plate 2 shows another example.

Figure 2 shows an example of silhouette interpolation. Note that the resulting silhouette has a different topology than any of the original data.

Plate 3 shows silhouette clipping used for efficient high quality rendering. In (a) the original high resolution mesh is shown. In (b) we show a low resolution approximation with 500 faces. In (c) the low resolution geometry is texture mapped using 20 precomputed texture views. In (d) we show the interpolated silhouette for this view. In (e), the interpolated silhouette is used to clip the low resolution mesh. In (f) the silhouette is also used to antialias the silhouette of the low resolution geometry.

In figure 10 we show timing performance on an SGI R5K, of our algorithm on the bunny data set. For the low resolution geometry we use 500 faces. The horizontal axis measures n , the (average) number of vertices in each of the silhouette contours of the silhouette map. The dot-dash line shows the time it takes to perform the silhouette interpolation for each frame. The dotted line shows the time it takes to interpolate the silhouette, and draw the low resolution using silhouette clipping. The solid line shows the time to interpolate, silhouette clip and apply projective textures. For comparison, we show timings for rendering high resolution geometry with n^2 faces. For evenly tessellated objects, it takes roughly n^2 faces to obtain a silhouette with n vertices. This is shown with a dashed line.

Plate 6 shows an example of our silhouette map simplification algorithm. We begin with 1024 evenly spaced views about the torus. When we have reached 128 views, the structure of the remaining star shaped polytope appears to be well tuned to the structure of silhouette changes for various directions.

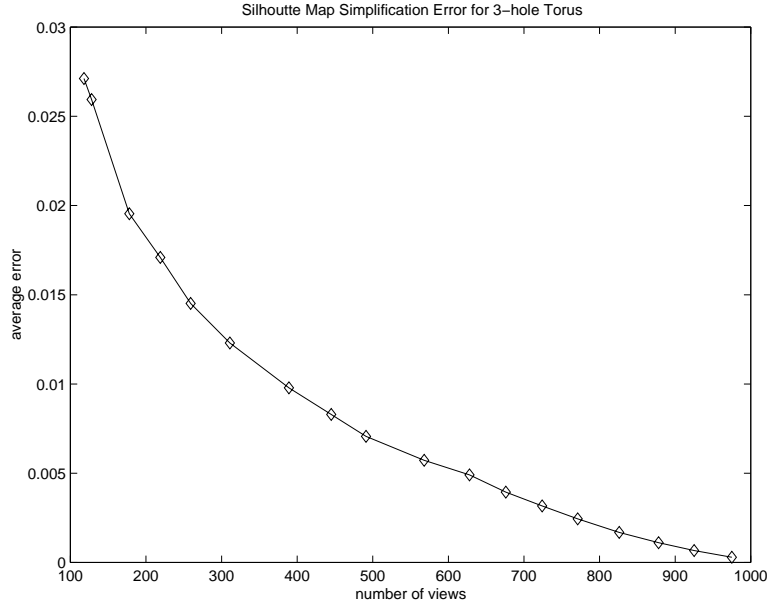


Figure 11: Silhouette map simplification error.

In figure 11, we show the performance of our simplification algorithm on the torus data set. The horizontal axis measures the number of views kept. Error is measured by comparing the original 1024 silhouette contours to those predicted by the simplified map. The number of misclassified pixels (exterior/interior) is measured. This number is divided by the entire number of pixels in the interior of the object for that view. This is summed up over all the views and divided by 1024. The simplification algorithm in conjunction with the silhouette interpolation method described produces a silhouette map with high fidelity and minimal storage overhead.

10 Discussion

We have introduced the framework of silhouette clipping, in which low-resolution geometry is rendered and clipped to a more accurate silhouette. During a preprocess, a silhouette map is formed by sampling the object silhouette from a discrete set of viewpoints. Interpolation of these silhouettes was made principled using a visual hull approximation of the model in a rectified epipolar setting. Topological changes between adjacent silhouettes can be handled properly by this algorithm. We reduced storage of the silhouette map through adaptive simplification.

To guarantee that the geometry be at least as large as the silhouette, we presented a technique for constructing a nested sequence of meshes, in which each coarser mesh completely encloses the original mesh.

Finally we reported on the rendering speedups possible using silhouette mapping.

Acknowledgements

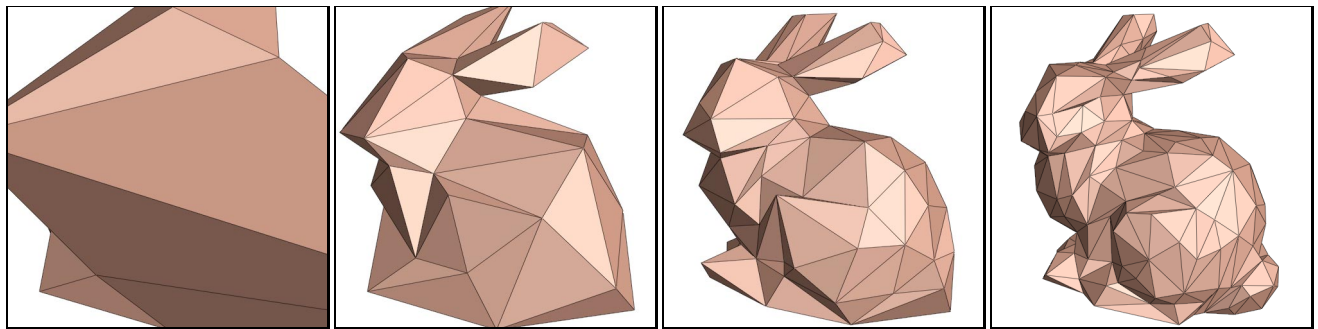
We would like to thank Aaron Isaksen for help with the Faro Arm, Peter-Pike Sloan for helpful input, and Julie Dorsey for making the MIT LCS graphics lab available to us. This work has been supported in part by NSF Career Awards 9703399, A Sloan research fellowship, and an IBM partnership award.

References

- [1] ADOBE SYSTEMS INC. *Postscript Language Reference Manual*, second ed. Addison Wesley, 1990.
- [2] B. VIJAYAKUMAR, D. KRIEBMAN, AND J. PONCE. structure and motion of curved 3d objects from monocular silhouettes. *Proc CVPR 96*.
- [3] BAJAJ, C., AND SCHIKORE, D. Error-bounded reduction of triangle meshes with multivariate data. *SPIE 2656* (1996), 34–45.
- [4] BLYTHE, D., GRANTHAM, B., NELSON, S., AND MCREYNOLDS, T. advanced graphics programming techniques using opengl.
- [5] BOYER, E., AND BERGER, M. 3d surface reconstruction using occluding contours. *IJCV* 22, 3 (1997), 219–233.
- [6] CIGNONI, P., MONTANI, C., ROCCHINI, C., AND SCOPIGNO, R. A general method for preserving attribute values on simplified meshes. In *Visualization '98 Proceedings* (1998), IEEE, pp. 59–66.
- [7] CIPOLLA, R., AND BLAKE, A. surface shape from the deformation of apparent contours. *IJCV* 9, 2 (1992), 83–112.
- [8] COHEN, J., MANOCHA, D., AND OLANO, M. Simplifying polygonal models using successive mappings. In *Visualization '97 Proceedings* (1997), IEEE, pp. 81–88.
- [9] COHEN, J., OLANO, M., AND MANOCHA, D. Appearance-preserving simplification. *Computer Graphics (SIGGRAPH '98 Proceedings)* (1998), 115–122.
- [10] DANIEL COHEN OR, DAVID LEVIN, AND AMIRA SOLOMOVICI. contour blending using warp guided distance field interpolation. *proc visualization 96*, 165–172.
- [11] DEBEVEC, P., C. TAYLOR, AND J. MALIK. modeling and rendering architecture from photographs. *SIGGRAPH 96*, 11–20.
- [12] DEBEVEC, P., Y. YU, AND G. BORSHUKOV. efficient view dependent image based rendering with projective texture mapping. *Eurographics rendering workshop 1998*.

- [13] GARLAND, M., AND HECKBERT, P. Surface simplification using quadric error metrics. *Computer Graphics (SIGGRAPH '97 Proceedings)* (1997), 209–216.
- [14] GIBLIN, P., AND WEISS, R. reconstruction of surfaces from profiles. *ICCV* (1987), 136–144.
- [15] GOOCH, A., GOOCH, B., SHIRLEY, P., AND COHEN, E. A non photorealistic lighting model for automatic technical illustration. *SIGGRAPH 98*.
- [16] GOOCH, B., SLOAN, P., GOOCH, A., SHIRLEY, P., AND RIESENFELD, R. Interactive technical illustration. *ACM Symposium on Interactive 3D graphics 1999* (1999).
- [17] GUÉZIEC, A. Surface simplification with variable tolerance. In *Proceedings of the Second International Symposium on Medical Robotics and Computer Assisted Surgery* (November 1995), pp. 132–139.
- [18] HECKBERT, P., AND GARLAND, M. Survey of polygonal surface simplification algorithms. In *Multiresolution surface modeling (SIGGRAPH '97 Course notes #25)*. ACM SIGGRAPH, 1997.
- [19] HOPPE, H. Progressive meshes. *Computer Graphics (SIGGRAPH '96 Proceedings)* (1996), 99–108.
- [20] HOPPE, H. View-dependent refinement of progressive meshes. *Computer Graphics (SIGGRAPH '97 Proceedings)* (1997), 189–198.
- [21] J. HUGUES. scheduled fourier volume morphing. *SIGGRAPH 92*, 43–46.
- [22] KOENDERINK, J. *Solid Shape*. MIT Press, 1990.
- [23] KOENDERINK, J. J. What does the occluding contour tell us about solid shape. *perception 13* (1984), 321–330.
- [24] KRISHNAMURTHY, V., AND LEVOY, M. Fitting smooth surfaces to dense polygon meshes. *Computer Graphics (SIGGRAPH '96 Proceedings)* (1996), 313–324.
- [25] LAURENTINI, A. the visual hull concept for silhouette based image understanding. *IEEE PAMI 16*, 2 (1994), 150–162.
- [26] LINDSTROM, P., AND TURK, G. Fast and memory efficient polygonal simplification. In *Visualization '98 Proceedings* (1998), IEEE, pp. 279–286.
- [27] LUEBKE, D., AND ERIKSON, C. View-dependent simplification of arbitrary polygonal environments. *Computer Graphics (SIGGRAPH '97 Proceedings)* (1997), 199–208.
- [28] M. LEVOY, AND P. HANRAHAN. light field rendering. *SIGGRAPH 96*, 31–42.
- [29] M. SHAPIRA, AND A. RAPPOPORT. shape blending using the star skeleton representation. *IEEE CG&A* (march 1995), 44–50.

- [30] MARKOSIAN, L., KOWALSKI, M., TRYCHIN, S., AND HUGUES, J. Real time non photo-realistic rendering. *SIGGRAPH 97* (1997).
- [31] MARUYA, M. Generating texture map from object-surface texture data. *Computer Graphics Forum (Proceedings of Eurographics '95)* 14, 3 (1995), 397–405.
- [32] MICROSOFT CORP. *Programming Windows*, fifth ed. Microsoft Press, 1998.
- [33] NEIDER, J., DAVIS, T., AND WOO, M. *OpenGL Programming Guide*. Addison-Wesley, 1993.
- [34] POTMESIL, M. generating octree models of 3d objects from their silhouettes in a sequence of images. *CVGIP* 40 (1987), 1–29.
- [35] S. GORTLER, R. GRZESZCZUK, R. SZELISKI, AND M. COHEN. The lumigraph. *SIGGRAPH 96*, 43–54.
- [36] S. POLLARD, AND S. HAYES. view synthesis by edge transfer with applications to the generation of immersive video objects. *Proc VRST 1998*, 91–98.
- [37] S. SEITZ, AND C. DYER. view morphing. *SIGGRAPH 96*, 21–30.
- [38] SEDERBERG, T., AND GREENWOOD, E. A physically based approach to 2d shape blending. *SIGGRAPH 92*, 25–34.
- [39] SEDERBERG, T., P. GAO, G. WANG, AND H. MU. 2d shape blending. *SIGGRAPH 93*, 15–18.
- [40] SEGAL, M., C. KOROBKIN, R. VAN WIDENFELG, J. FORAN, AND P HAEBERLI. fast shadows and lighting effects using texture mapping. *SIGGRAPH 92*, 249–252.
- [41] SOUCY, M., GODIN, G., AND RIOUX, M. A texture-mapping approach for the compression of colored 3D triangulations. *The Visual Computer* 12 (1986), 503–514.
- [42] XIA, J., AND VARSHNEY, A. Dynamic view-dependent simplification for polygonal models. In *Visualization '96 Proceedings* (1996), IEEE, pp. 327–334.

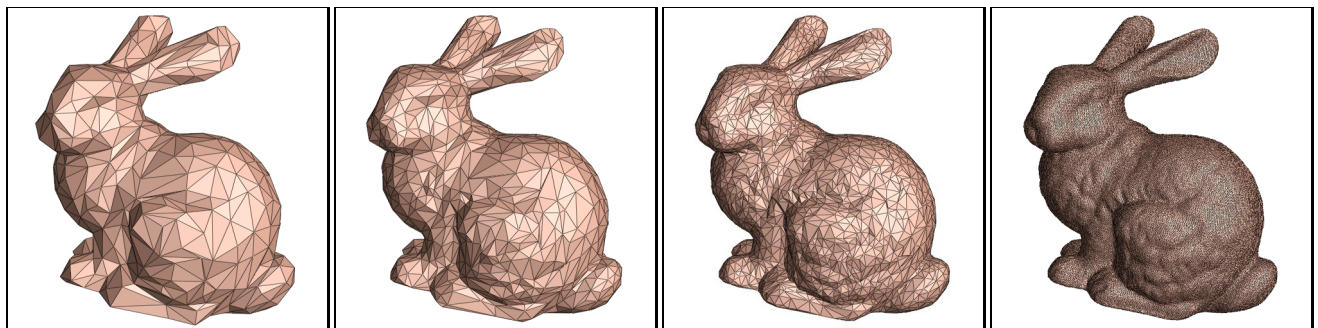


(a) M^0 (38 faces)

(b) M^{31} (100 faces)

(c) M^{81} (200 faces)

(d) M^{231} (500 faces)



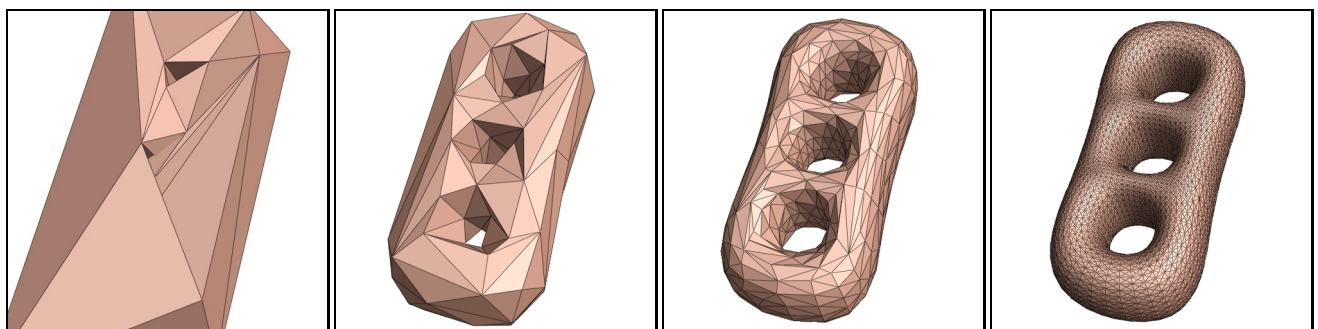
(e) M^{481} (1,000 faces)

(f) M^{981} (2,000 faces)

(g) M^{2481} (5,000 faces)

(h) Original mesh M^n

Plate 1: Example of progressive hull construction. The original mesh $M^{n=34818}$ has 69,674 faces.



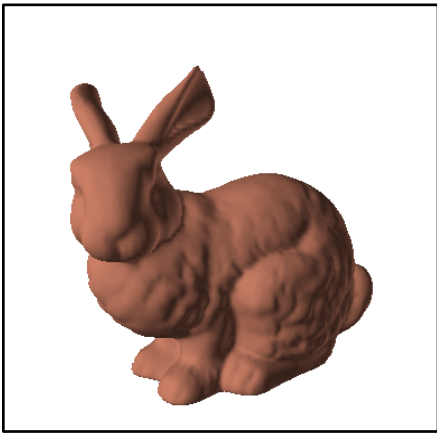
(a) M^0 (62 faces)

(b) M^{69} (100 faces)

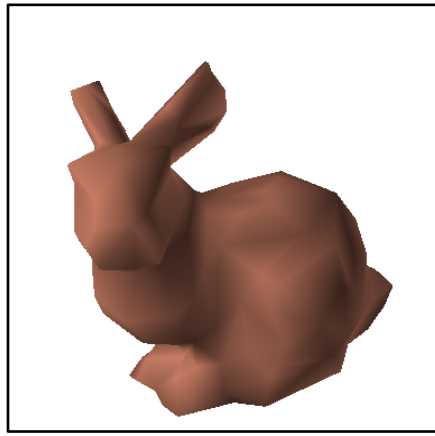
(c) M^{469} (1,000 faces)

(d) M^{5857} (11,776 faces)

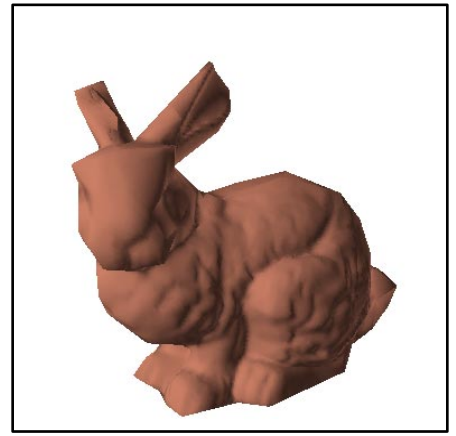
Plate 2: Another example of progressive hull construction.



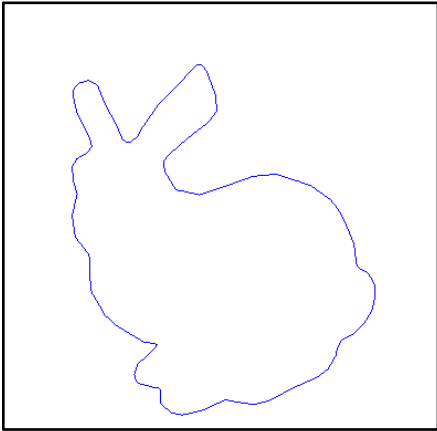
(a) Original Mesh



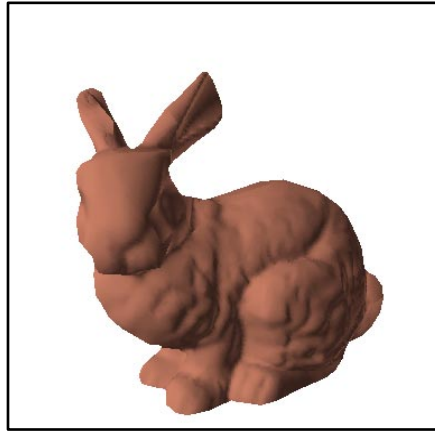
(b) 500 faces



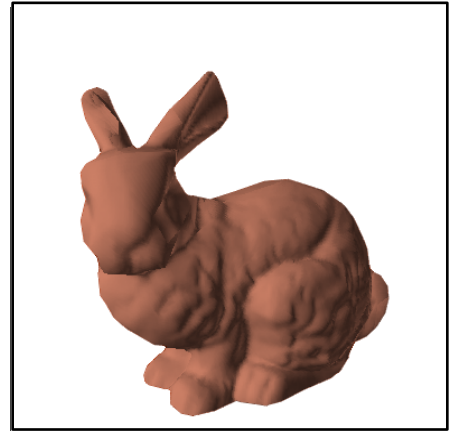
(c) 500 faces with texture



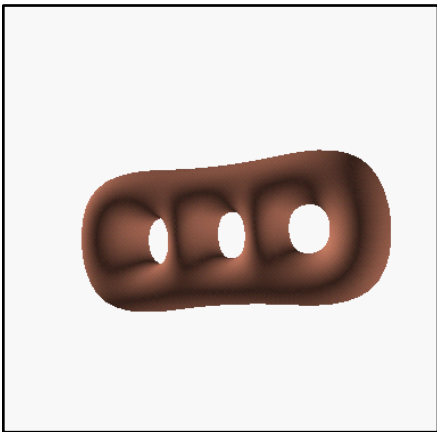
(d) Synthesized silhouette



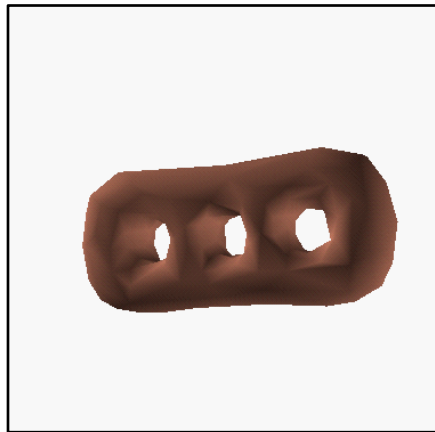
(e) 'c' with silhouette clipping



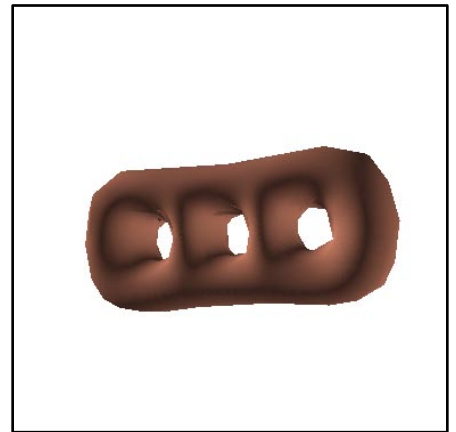
(f) 'c' with soft silhouette clipping



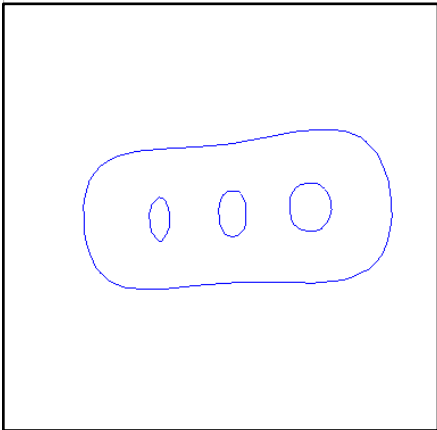
(a) Original Mesh



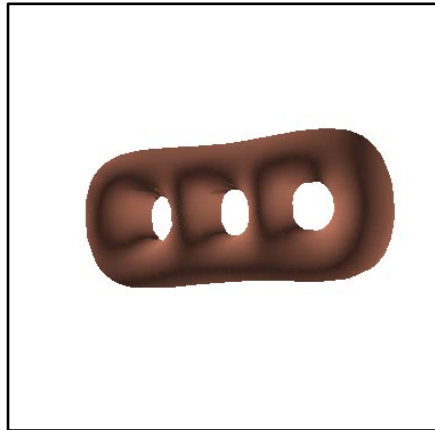
(b) 500 faces



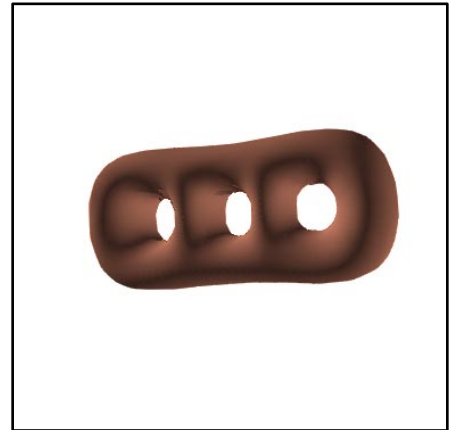
(c) 500 faces with texture



(d) Synthesized silhouette



(e) 'c' with silhouette clipping



(f) 'c' with soft silhouette clipping

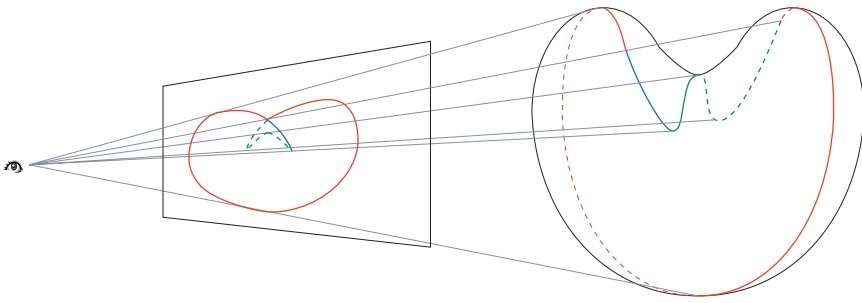


Plate 4: Contour generator on object.

Apparent contour on image plane. Visible apparent contour in red/blue. External visible apparent contour in red.

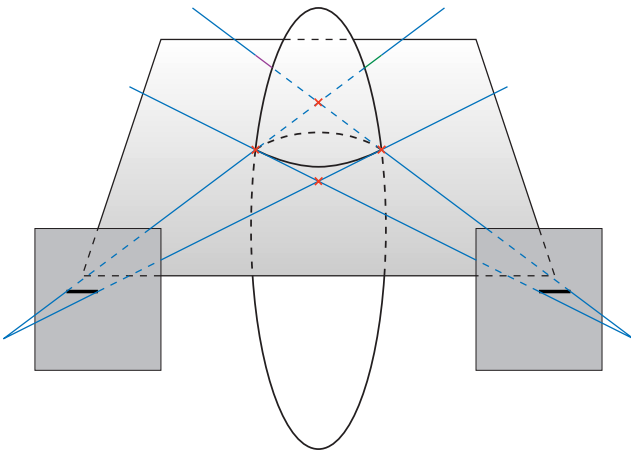
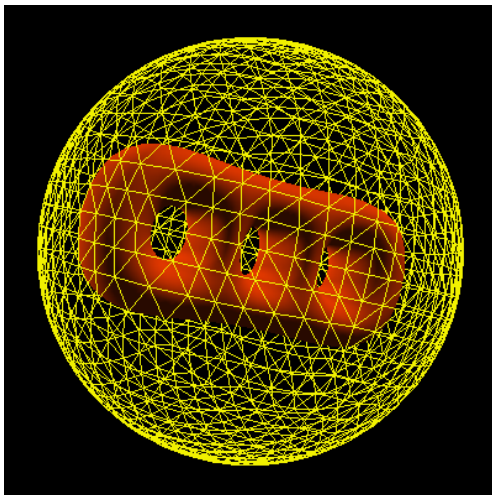
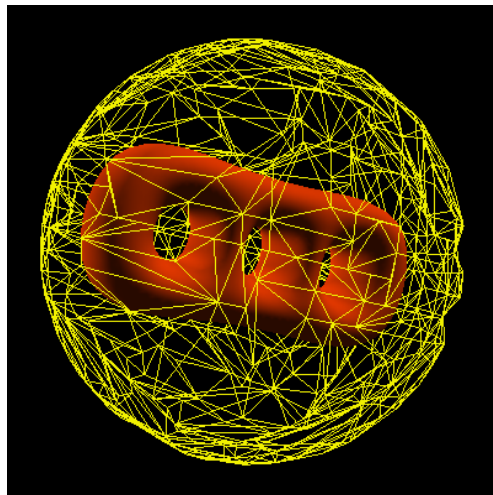


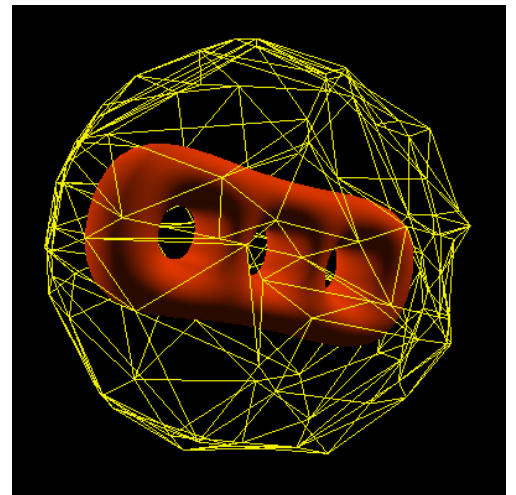
Plate 5: Epipolar decomposition



(a)1024 views



(b)491 views



(c)128 views

Plate 6: Simplification of silhouette map